Influence of modification on microstructure degradation of AlSi12 alloy exposed to the corrosion environment

Kozina, Franjo; Zovko Brodarac, Zdenka

INFLUENCE OF MODIFICATION ON MICROSTRUCTURE DEGRADATION OF AlSi12 ALLOY EXPOSED TO THE CORROSION ENVIRONMENT

Franjo KOZINA, Zdenka ZOVKO BRODARAC

University of Zagreb Faculty of Metallurgy, Sisak, Croatia, EU, fkozin@simet.hr, zovko@simet.hr

Abstract

The corrosion resistance of aluminum-silicon (Al-Si) foundry alloys is a result of microstructure development influenced by melt treatment and solidification. As a part of the main eutectic (α_{Al} + β_{Si}), β_{Si} particles are cathodic with respect to the α_{Al} matrix enabling micro-galvanic couple formation and localized corrosion. Despite its high polarization and low current density, increase in the eutectic (α_{Al} + β_{Si}) will contribute to the microstructure degradation of an alloy in corrosive environment. The research was performed in order to estimate the influence of eutectic β_{Si} particles size on the microstructure degradation of AlSi12 alloy with mixed morphology of eutectic (α_{Al} + β_{Si}). The results of light microscopy indicated preferred initiation and progress of cavities involving modified eutectic (α_{Al} + β_{Si}) with eutectic β_{Si} particles of smaller average particle size. The unmodified eutectic (α_{Al} + β_{Si}) with lamellar morphology and dendrites of primary α_{Al} phase were not visually affected by degradation. The average cavity size and pH value of the solution increase with the increasing exposure time, while microstructure degradation rate decreases.

Keywords: AlSi12, eutectic modification, particle size, corrosion environment, microstructure degradation

1.   INTRODUCTION

The corrosion resistance of aluminum-silicon (Al-Si) foundry alloy derives from chemical composition, value of secondary dendrite arm spacing (SDAS) and anodic or cathodic behavior of the main or secondary phase components [1]. Although, size of the SDAS has a direct influence on mechanical properties, it is not clear if decrease in the SDAS improves resistance to microstructure degradation in corrosive environment. In order to understand microstructures tendency towards degradation, SDAS needs to be correlated with phase distribution into the interdendritic region and its anodic/cathodic behavior with respect to the α_{Al} matrix [2]. As a part of the main eutectic (α_{Al} + β_{Si}), β_{Si} particles are cathodic with respect to the α_{Al} matrix causing the formation of micro-galvanic couples and localized corrosion phenomena [3]. Even due the effect of β_{Si} particles on microstructure degradation is minimal, due to its high polarization and low current density, increase of eutectic (α_{Al} + β_{Si}) ratio in microstructure will have deleterious effect on the alloy's microstructure [4].

The chemical modification of Al-Si foundry alloys influences eutectic (α_{Al} + β_{Si}) solidification and leads to structural transformation of the eutectic β_{Si} phase from course lamellar to fine fibrous morphology. This structural refinement, caused by the addition of modifiers, increases circularity and reduces particle size and aspect ratio of modified eutectic β_{Si} phase [5]. Consequently, modification has direct influence on fracture surface geometry as well as beneficial influence on ductility, toughness, tensile strength, and elongation [6].

The goal of the research is to estimate the influence of β_{Si} particle size and distribution on the microstructure degradation of eutectic AlSi12 alloy in the corrosive environment. The applied method simulates various types of outdoor services, especially in marine and automotive applications. The progress of the accelerated corrosion process and its impact on the macrostructure and microstructure will be estimated visually using light microscopy.

2.   MATERIALS AND METHODS

The synthesis of eutectic AlSi12 alloy began by remelting of the AlSi12 block followed by chemical composition augmenting through the additions of AlSi50%, AlTi10 and AlMn master alloys. After stirring with argon and chemical degasing, the alloy was modified by adding metallic sodium packed in vacuum sealed aluminum can. In order to obtain modified and unmodified morphology of eutectic β_{Si} particles, the samples were taken 10 min (sample 1) and 60 min (sample 2) after the addition of the modifier by pouring into a permanent steel mould. Approximately 2 min after pouring the samples were quenched in water.

Chemical composition of the synthesized alloy was determined spectroscopically using SPECTRO MAX x LMM 04 spectrometer.

The samples for metallographic analysis were prepared using standard grinding and polishing techniques. The samples for macrostructural analysis were etched using Poulton's etching solution. The macrostructure was observed using stereo microscope Olympus SZ11.

The samples for light microscopy were etched in 0.5 % aqueous hydrofluoric acid solution. The microstructure was analyzed using the Olympus GX51 inverted metallographic microscope equipped with AnalySIS Materials Research Lab software support. Application of the particle analysis enabled particle count and area classification of eutectic β_{Si} particles. Five micrographs per sample were analyzed by setting threshold at the binary images.

Before exposure to the corrosive environment, the samples were grinded and mounted in inert resin. The mounting was performed in order to prevent spontaneous degradation from all sides.

The solution for the corrosion testing was obtained by dissolving 234 g of sodium chloride (NaCl) and 50 g of potassium nitrate (KNO$_3$) in water. Afterwards, 6.3 ml of HNO$_3$ were added and the solution was diluted to 1 l by adding distilled water. The obtained solution had the apparent pH of 0.4. The samples were immersed in the solution for 5, 24, 48 and 72 h. After words, the samples were neutralized in concentrated HNO$_3$, rinsed in distilled water, alcohol and dried in hot air. The Laboratory pH Meter inoLab LeV1 was used to measure changes in pH of the solutions after the samples were removed.

By calculating loses of mass with respect to exposure time, the microstructure degradation rate was calculated.

The macrostructure was analysed on the exposed surface of the samples, while microstructural analysis was performed on the cross-section of the samples after standard metallographic preparation and etching in 0.5 % aq HF solution. Analysis of the cross-section enabled cavity depth measurements.

3.   RESULTS AND DISCUSSION

The results of chemical analysis are given in **Table 1**.

Table 1 Chemical composition of the produced alloy (wt%)

Si	Fe	Mn	Mg	Ni	Sn	Ti	Na	Al
12.9	0.151	0.077	0.065	0.006	0.065	0.081	0.014	Balance

The chemical composition of the produced alloy is in accordance with EN 1706:2010 for EN AC 4410 (EN AC AlSi12) alloys. The addition of Na is sufficient to fully modify eutectic (α_{Al} + β_{Si}) from course lamellar to fine fibrous morphology.

The macrostructure and microstructure of the samples are given in **Figure 1**.

a)

b)

c)

d)

e)
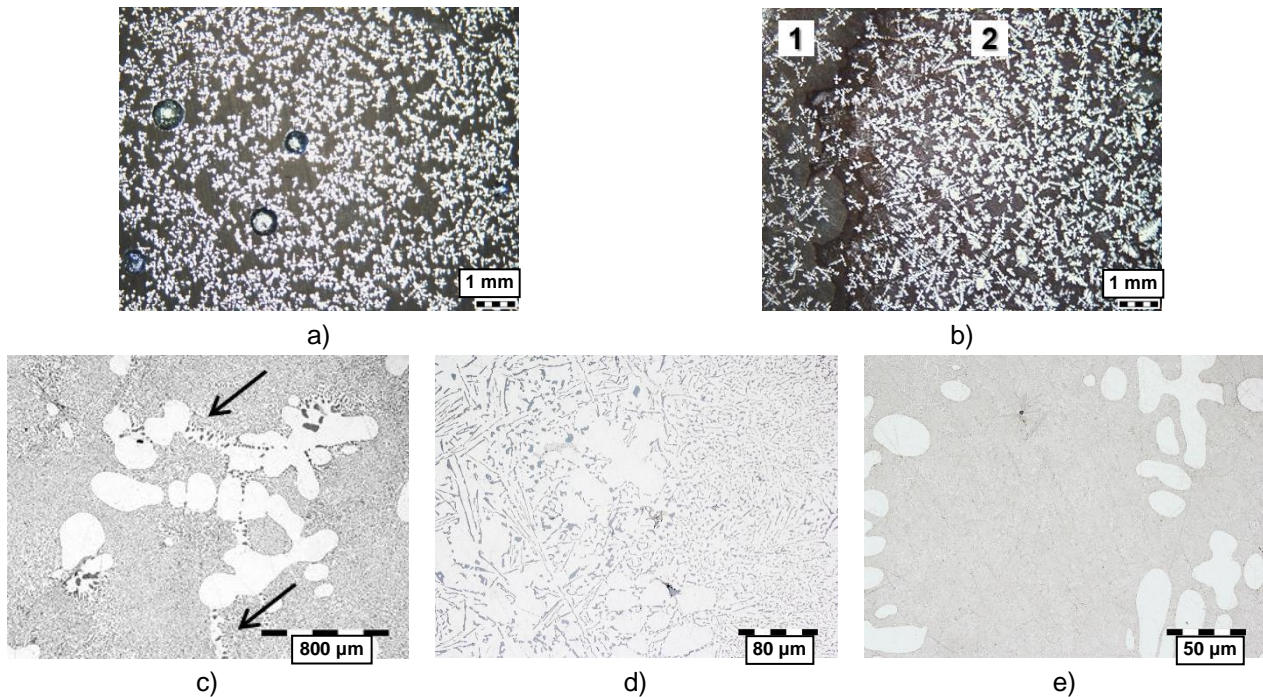
Figure 1 Micrographs of: a) macrostructure of the sample 1, b) macrostructure of the sample 2, c) microstructure of the sample 1, d) microstructure of the sample 2 in the area 1, e) microstructure of the sample 2 in the area 2

The macrostructure of the samples consists of a dendritic network of primary α_{Al} phase (**Figures 1 a, b**, bright areas) and interdendritic areas filled with eutectic (α_{Al} + β_{Si}) (**Figures 1 a, b**, dark areas). The macrostructure of the sample 2 also reveals the presence of solid-liquid interface with growth direction from surface to the center of the sample. The quenching of the sample enabled formation of central zone (**Figure 1 b**, zone 2) and surface zone with average thickness of 2.69 mm (**Figure 1 b**, zone 1). In the sample 1 eutectic (α_{Al} + β_{Si}) is fully modified with fine fibrous morphology (**Figure 1 a**). Due to the over modification with Na, the coarsening of the eutectic β_{Si} particles and the overgrowth of the α_{Al} matrix can be seen at the grain boundaries (**Figure 1 c**). The microstructural analysis of the sample 2 indicates the difference in eutectic (α_{Al} + β_{Si}) morphology between the zones. The surface zone eutectic (α_{Al} + β_{Si}) has lamellar morphology (**Figure 1 d**), while the eutectic (α_{Al} + β_{Si}) in central zone is fully modified (**Figure 1 e**).

The results of particle analysis are given in **Table 2**.

Table 2 Results of particle analysis

Sample	Zone	Particle count (µm)	Particle area (µm)	Average particle size (µm)
1	/	3230.6	6739.36	2.09
2	surface	1400.2	7465.05	5.33
2	central	1911.6	1906.11	1.00

The results of the particle analysis indicate the highest particle count in sample 1 with average particle size of 2.09 µm (**Table 1**). The lowest particle count was measured in the surface zone of sample 2 with largest average particle size of 5.33 µm. The central zone of sample 2 has the smallest average particle size of 1.0 µm (**Table 1**).
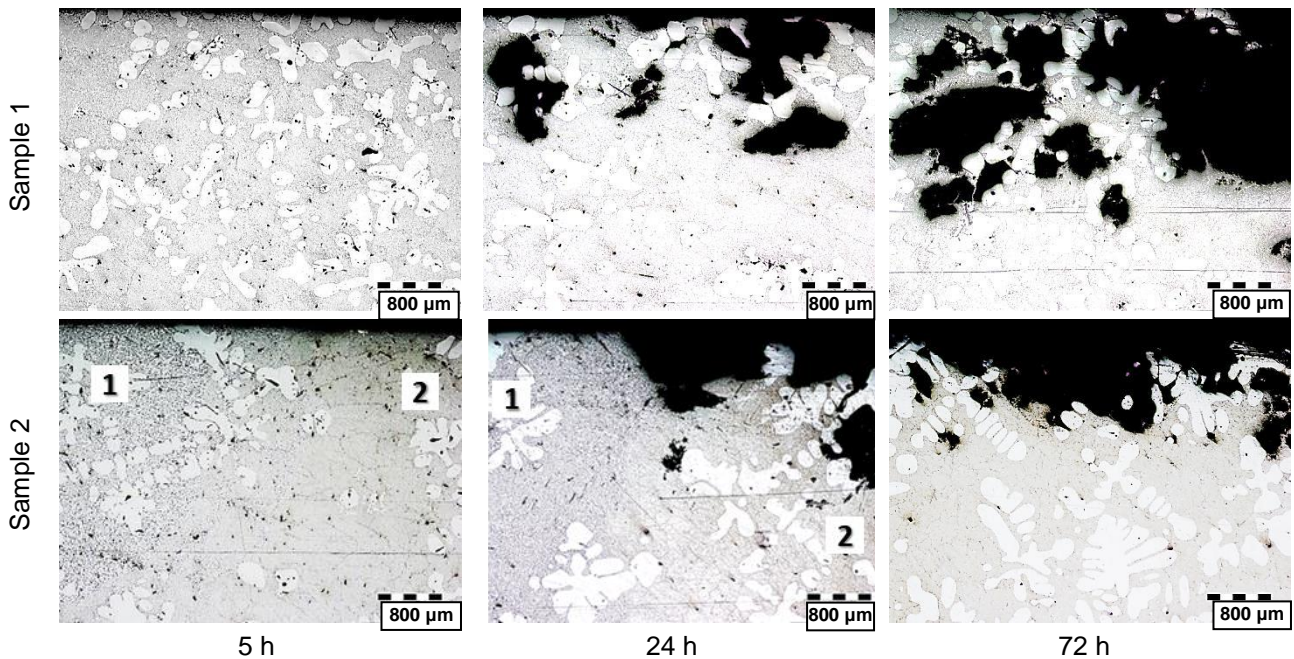
The example of the samples macrostructure after 48 h of exposure is given in **Figure 2**.

a)

b)
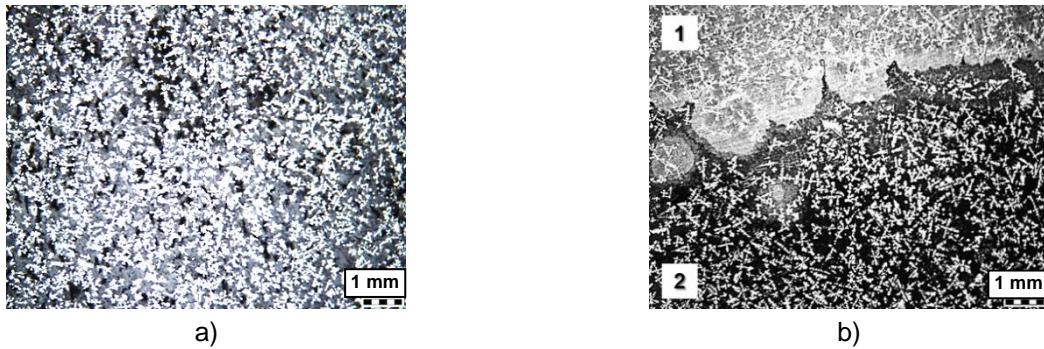
Figure 2 Macrostructure of samples at the magnification of 12.5 X:
a) Sample 1, b) Sample 2

During 48 h of exposure the microstructure degradation of sample 1 comprehended cavities formation in the interdendritic areas of primary α_{Al} phase (**Figure 2 a,** black areas). Exposure of sample 2 to the corrosive environment indicated quenched solid-liquid interface and small spherical colonies (**Figure 2 b**). The central zone of the sample 2 shows more significant microstructural degradation compared to the surface zone (**Figure 2 b,** black areas).

The microstructure of the samples after 5, 24 and 72 h exposure is shown in **Figure 3**.

Figure 3 Microstructure of the samples after 5, 24, 72 h exposure to the corrosive environment

The cross-section of the sample 1, 5 h after the exposure shows negligible microstructural degradation. The cavities can be seen 24 and 72 h after the beginning of the testing. The cavities initiate at the exposed surface and progress deeper into the material affecting the eutectic (α_{Al} + β_{Si}) located in the interdendritic network of primary α_{Al} phase (**Figure 3**, sample 1). The microstructure of the sample 2 after 5 h of exposure shows the lack of cavities at the solid-liquid interface. However, the small cavities forming at the surface of the sample can be found in central zone. The microstructure of the sample after 24 h of exposure shows presence of cavities at the solid-liquid interface progressing into the central zone with average size of eutectic β_{Si} particle 1.00 µm (**Table 2**). In next 72 h, the cavities progress deeper into the material affecting the modified eutectic

(α_{Al} + β_{Si}). The unmodified eutectic (α_{Al} + β_{Si}) with average size of eutectic β_{Si} phase particle 5.33 μm (**Table 2**) is not significantly affected by the corrosion processes (**Figure 3**, sample 2).

The average cavity depth and rate of the microstructure degradation are shown in **Figure 4**, while the changes in pH value are given in **Table 3**.
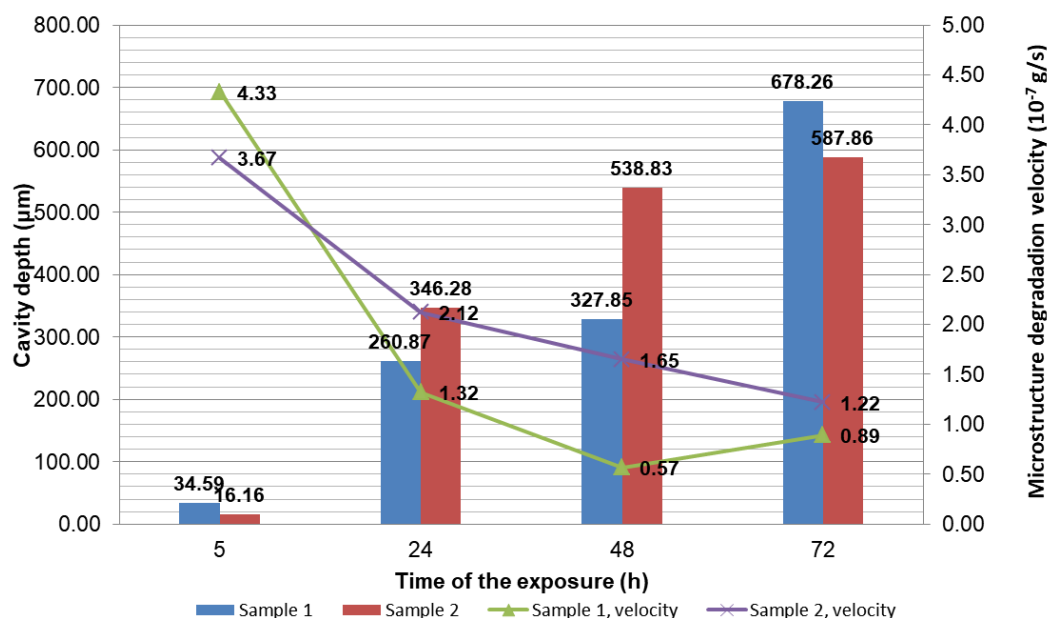
Figure 4 The average cavity depth and microstructure degradation rate

Table 2 The changes in pH value per sample and corrosion exposure time

Sample	Corrosion exposure time (h)			
	5	24	48	72
1	0.38	0.53	0.88	1.14
2	0.35	0.65	1.31	1.59

During the first 5 h the cavities with the average cavity size of 34.59 μm can be observed at the surface of the sample 1. The cavities form with the rate of 4.33·10^{-7} g/s (**Figure 4**). The solution pH value decreases to 0.38 (**Table 2**). After 24 h the cavities with the average cavity size of 280.87 μm were formed with rate of 1.32·10^{-7} g/s (**Figure 4**). The pH value of the solution increases to 0.53 (**Table 2**). After 48 h of exposure the microstructure degradation rate decreases to 0.57·10^{-7} g/s while average cavity size increases to 328 μm (**Figure 4**). The solution pH value increases to 0.88 (**Table 2**). Towards the end of the exposure the microstructure degradation rate increases to 0.89·10^{-7} g/s resulting in the cavity formation with average cavity size of 678 μm (**Figure 4**). The pH value increases to 1.14.

During the first 5 h the cavities with the average cavity size of 16 μm were formed at the surface of the sample 2. The cavities form with the rate of 3.67·10^{-7} g/s (**Figure 4**). The solution pH value decreases to 0.35 (**Table 2**). After 24 h the cavities with the average cavity size of 346 μm were formed with rate of 2.12·10^{-7} g/s (**Figure 4**). The pH value of the solution increases to 0.65 (**Table 2**). After 48 h of exposure the microstructure degradation rate decreases to 1.65·10^{-7} g/s while average cavity size increases to 539 μm (**Figure 4**). The solution's pH value increases to 1.31 (**Table 2**). Towards the end of the exposure the microstructure degradation rate decreases to 1.22·10^{-7} g/s resulting in the cavity formation with average cavity size of 588 μm (**Figure 4**). The pH value increases to 1.59.

The results of the measurements indicate the constant increase in average cavity size and pH value with the increase in corrosion exposure time. On the other hand the microstructure degradation rate decreases with the increase in exposure time. Compared to sample 2, the sample 1 shows more significant microstructure degradation and higher corrosion rate at 5 h and 72 h.

4. CONCLUSION

In order to estimate the influence of eutectic β_{Si} particle size and distribution on the microstructure degradation in corrosive environment, AlSi12 alloy with modified and unmodified morphology of eutectic ($\alpha_{Al} + \beta_{Si}$) was produced.

The microstructural analysis indicated the formation of cavities in both samples. The cavities initiated at the exposed surface and progressed deeper into the material affecting the eutectic ($\alpha_{Al} + \beta_{Si}$). The most significant microstructure degradation was observed in the central zone of the sample 2 with the smallest average particle size of β_{Si} particle 1.0 μm. On the other hand, the unmodified eutectic ($\alpha_{Al} + \beta_{Si}$) with average particle size of β_{Si} particle 5.3 μm, located in surface zone of the sample 2, was not visually affected by the microstructural degradation. The dendritic network of primary α_{Al} phase was not visually affected by the microstructural degradation. The average cavity size increases with the increase in the exposure time. The microstructure degradation rate decreases with the increase in pH value.

Performed investigation indicated that shorter modification (10 min) shortened the solidification interval and encouraged the natural solidification conditions (without solid-liquid interface). Those conditions comprehend homogeneous microconstituents distribution, smaller in size (Sample 1). As a part of eutectic phase, fibrous β_{Si} was more resistant to corrosion environment till 24 h of exposure, according to cavity depth measurement.

ACKNOWLEDGEMENTS

REFERENCES

[1]   ŠĆEPANOVIĆ, J., ASANOVIĆ, V., RADONJIĆ, D., VUKSANOVIĆ, D., HERENDA, S., KORAĆ, F. BIKIĆ, F. Mechanical properties and corrosion behavior of Al-Si alloys for IC engine. *Journal of the Serbian Chemical Society*. 2019, vol. 84, no. 5, pp. 503–516.

[2]   BERLANGA, C., BAKEDANO, A., DE CIRIZA, A. PEREZ RIVERO, P. J., MENDEZ, S., RODRIGUEZ, R., NIKLAS, A. Evaluation of the corrosion resistance of a new AlSi10MnMg(Fe) secondary alloy. *Materials Today: Proceedings*, 2018, vol. 10, pp. 312–318.

[3]   ARTHANARI, S., JANG, J. C., SHIN, K. S. Corrosion performance of high pressure die-cast Al-Si-Mg-Zn alloys in 3.5 wt% NaCl solution. *Journal of Alloys and Compounds*. 2018, vol. 783, pp. 494–502.

[4]   DUYGUN, I. K., HAPÇI AĞAOĞLU, G., DISPINAR, D., ORHAN, G. Time-dependent corrosion properties of Sr-modified AlSi9 alloy analyzed by electrochemical techniques. *Journal of Alloys and Compounds.* 2019, vol. 803, pp. 786–794.

[5]   STJOHN, D., MCDONALD, S., DARLAPUDI, A. A new perspective on the nucleation, growth morphology and modification of the silicon phase during the formation of eutectic Al-Si grains. *JoM*. 2019, vol. 71, no. 1, pp. 391–396, 2019.

[6]   KRUGLOVA, A., ROLAND, M., DIEBELS S., DAHMEN, T., SLUSALLEK, P., MÜCKLICH, F. Modelling and characterization of ductile fracture surface in Al-Si alloys by means of Voronoi tessellation. *Materials Characterization*. 2017, vol. 131, pp. 1–11.